

Effect of nonlinear dissipation on the basin boundaries of a driven two-well or catastrophic single-well Modified Rayleigh-Duffing Oscillator

C. H. Miwadinou*, A. V. Monwanou† and J. B. Chabi Orou‡

Abstract

This paper considers effect of nonlinear dissipation on the basin boundaries of a driven two-well Modified Rayleigh-Duffing Oscillator where pure and unpure quadratic and cubic nonlinearities are considered. By analyzing the potential an analytic expression is found for the homoclinic orbit. The Melnikov criterion is used to examine a global homoclinic bifurcation and transition to chaos in the case the of our oscillator. It is found the effect of unpure quadratic parameter and amplitude of parametric excitation on the critical Melnikov amplitude μ_{cr} . Finally, we examine carefully the phase space of initial conditions in order to analyze the effect of the nonlinear damping, and particular how the basin boundaries become fractalized.

keywords: Catastrophic single-well potential, two-well potential, modified Rayleigh-Duffing oscillator, melnikov criterion, bifurcation, chaotic behavior, basin boundaries.

1 Introduction

The Rayleigh oscillator is one canonical example of self-excited systems. However, generalizations of such systems, such as the Rayleigh–Duffing oscillator, have not received much attention. The presence of a pure and unpure quadratic and cubic terms makes the Rayleigh–Duffing oscillator a more complex and interesting case to analyze. This oscillator is used to modelize the following phenomenon: a El Niño Southern Oscillation (*ENSO*) coupled tropical ocean-atmosphere weather phenomenon in which the state variables are temperature and depth of a region of the ocean called the thermocline (where the annual seasonal cycle is the parametric excitation and the model exhibits a Hopf bifurcation in the absence of parametric excitation), a *MEMS* device consisting of a $30\mu m$ diameter silicon disk which can be made to vibrate by heating it with a laser beam resulting in a Hopf bifurcation (where the parametric excitation is provided by making the laser beam intensity vary periodically in time) etc. [16] and [18].

The behavior of Rayleigh-Duffing oscillator with periodic forcing and/or parametric excitations has been investigated extensively by many researchers. For instance,

*clement.miwadinou@imsp-uac.org, hodevewan@yahoo.fr

†movins2008@yahoo.fr

‡Author to whom correspondence should be addressed: jchabi@yahoo.fr

in their work, the siewe siewe and their collaborators [20] have studied the nonlinear response and suppression of chaos by weak harmonic perturbation inside a triple well 6–Rayleigh oscillator combined to parametric excitations. Three years ago, Siewe Siewe and al.[2] investigated the effect of the nonlinear dissipation on the boundaries of a driven two-well Rayleigh-Duffing oscillator and in other paper [3], the same authors focussed their analyze on the occurrence of chaos in a parametrically driven extended Rayleigh oscillator with three-well potential. However, in many situations, the nonlinear dynamics dominates the behavior of physical systems giving rise to multi-stable potentials or catastrophic monostable potentials. The authors in Refs. [2, 3] and [20] showed with a rigorous theoretical consideration that the resonant parametric perturbation can remove chaos in low dimensional systems. They confirmed this prediction with numerical simulations. It is interesting to note that there is a situation analyzed in [21], where Melnikov analysis is applied to a nonlinear oscillator which can behave as a one-well oscillator, a two-well oscillator or three-well oscillator by simply modifying one of its parameters, which acts as a symmetry-breaking mechanism. Therefore, the chaotic behavior using the parametric perturbation in the modified Rayleigh–Duffing oscillator with a two-well potential still needs to be investigated further. Another good example is constituted by the generalized perturbed pendulum [22]. Our aim is to make a contribution in the study of the transition to chaos in the modified Rayleigh–Duffing oscillator by using the Melnikov theory, and then see how the fractal basin boundaries arise and are modified as the damping coefficient is varied. The last part of this work consists of a numerical investigation of the strange attractor at parameter values which are close to the analytically predicted bifurcation curves. In particular, the case of the two-well potential is considered.

The paper is organized as follows. In the next section, after describing the model, analyzing of the model, and some comparison with the simple Rayleigh-Duffing oscillator, the conditions for the existence of chaos are thoroughly analyzed. A convenient demonstration of the accuracy of the method is obtained from the fractal basin boundaries, and this is discussed in Section 4. We conclude in the last section. In the appendix *A* we show the Melnikov integration procedures in details.

2 Description and analysis of the model

In this paper, we examine the dynamical transitions in parametric and periodically forced self-oscillating systems containing the cubic terms in the restoring force and the pure and hybrid quadratic and cubic in nonlinear damping function as follows:

$$\begin{aligned} \ddot{x} + \epsilon\mu(1 - \dot{x}^2)\dot{x} + \epsilon\beta\dot{x}^2 + \epsilon k_1\dot{x}x + \epsilon k_2\dot{x}^2x + (\gamma + \alpha \cos \Omega t)x \\ + \lambda x^3 = F \cos \Omega t, \end{aligned} \quad (1)$$

where $\epsilon, \mu, \beta, k_1, k_2, \gamma, \lambda, F$ and Ω are parametrs. Physically, μ, k_2, β and k_1 represent respectively pure, unpure cubic and pure, unpure quadratic nonlinear damping coefficient terms, α and F are the amplitudes of the parametric and external periodic forcing, and $\sqrt{\gamma}$ and Ω are respectively natural and external forcing frequency. Moreover λ characterize the intensity of the nonlinearity and ϵ is the nonlinear damping parametr control. The nonlinear damping term corresponds to the Modified Rayleigh oscillator, while the nonlinear restoring force corresponds to the Duffing oscillator, hence its name Modified Rayleigh-Duffing oscillator.

In this section, we derive the fixed points and the phase portrait corresponding to the system Eq. (1) when it is unperturbed. If we let $\epsilon = \alpha = F = 0$, Eq. (1) is

considered as an unperturbed system and can be rewritten as

$$\dot{x} = y, \quad \dot{y} = -\gamma x - \lambda x^3, \quad (2)$$

which corresponds to an integrable Hamiltonian system with the potential function given by

$$V(x) = \frac{1}{2}\gamma x^2 + \frac{1}{4}\lambda x^4, \quad (3)$$

whose associated Hamiltonian function is

$$H(x, y) = \frac{1}{2}y^2 + \frac{1}{2}\gamma x^2 + \frac{1}{4}\lambda x^4. \quad (4)$$

From Eqs. (2) and (4), we can compute the fixed points and analyze their stabilities.

- If $\gamma > 0, \lambda > 0$ or $\gamma < 0, \lambda < 0$, the system have one fixed point $(0, 0)$ which is a center.
- For $\gamma > 0, \lambda < 0$, there are three fixed points: two saddles connected by two heteroclinic orbits and one center. The potential defined by Eq. (3) has two-well (see Fig. 1(b)).
- For $\gamma < 0, \lambda > 0$, there are three fixed points: two saddles connected by two heteroclinic orbits and one center. The potential defined by Eq. (3) has catastrophic sigle-well (see Fig. 1(a)).

Therefore, depending on the values of the external excitation, the system can escape over the potential barrier and dramatically suffers an unbounded motion. Fig. represents the corresponding phase portraits between the unforced Rayleigh–Duffing oscillator and the unforced Modified Rayleigh–Duffing oscillator, respectively with single-well (left) and two-well (right) conditions.

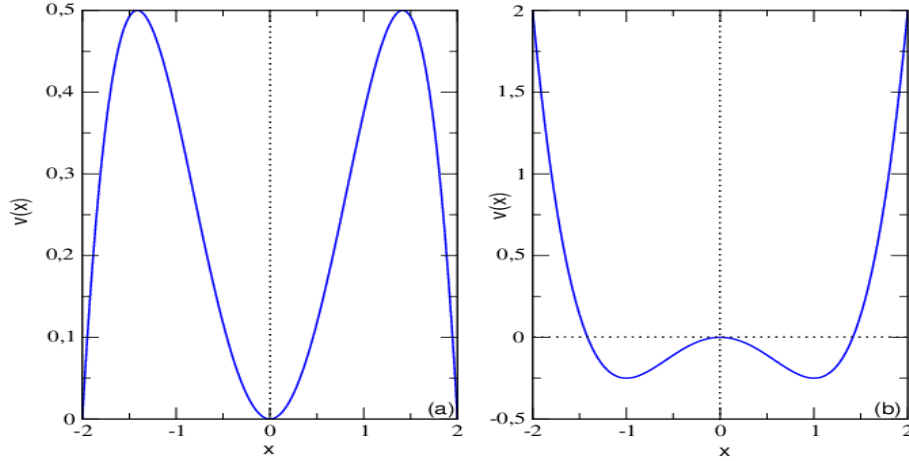


Figure 1: (a) The catastrophic single well potential of the unperturbed system (4); b The two-well potential function of the unperturbed system (4).

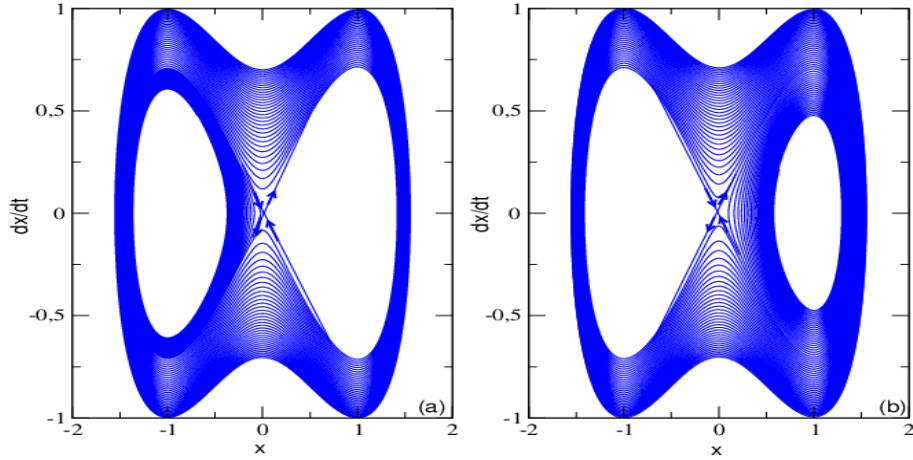


Figure 2: (a) Phase portrait of the unforced Rayleigh-Duffing oscillator with $\gamma = -1, \lambda = 1, \alpha = 0, \beta = 0, \mu = 0.2, \epsilon = 0.1, k_1 = 0, k_2 = 0$; (b) Phase portrait of the unforced Modified Rayleigh-Duffing oscillator with $\gamma = -1, \lambda = 1, \alpha = 0.5, \beta = 0.5, \mu = 0.2, \epsilon = 0.1, k_1 = 0.5, k_2 = 0.5$

3 Taming chaotic behavior in the Modified Rayleigh-Duffing oscillator

In this section, we discuss the chaotic behavior of the system

$$\begin{aligned} \ddot{x} + \epsilon\mu(1 - \dot{x}^2)\dot{x} + \epsilon\beta\dot{x}^2 + \epsilon k_1\dot{x}x + \epsilon k_2\dot{x}^2x + (\gamma + \alpha \cos \Omega t)x \\ + \lambda x^3 = F \cos \Omega t, \end{aligned} \quad (5)$$

where $\mu, k_1, \beta, k_2, \gamma, \alpha, \lambda, \Omega$ and F are assumed to be small parameters. Hence, our dynamical system may be written as

$$\begin{aligned} \dot{x} = y, \quad \dot{y} = -\gamma x - \alpha x \cos \Omega t - \lambda x^3 - \epsilon\mu(1 - \dot{x}^2)\dot{x} - \epsilon\beta\dot{x}^2 - \\ \epsilon k_1\dot{x}x - \epsilon k_2\dot{x}^2x + F \cos \Omega t, \end{aligned} \quad (6)$$

where $F = \epsilon F$

When the perturbations are added, the homoclinic orbit might be broken transversely. And then, by the smale-Birkoff Theorem[19], horseshoe type chaotic dynamics may appear. It is well known, that the predictions for the appearance of chaos are limited and only valid for orbits starting at points sufficiently close to the separatrix. On the other hand it constitutes a first order perturbation method. Although the chaos does not manifest itself in the form of permanent chaos, and some sorts of transient chaos may showup. Hower, it manifest itself in terms of fractal basin boundaries, as it was shown by[20]. We start our analysis form the unperturbed Hamiltonian Eq. (4). The potential $V(x)$ Eq. (3) has the local peak (Fig. 1 (b)) or local antipeak (see Fig. 1 (a)) at the saddle point $x = 0$. Esistence of this point with a horizontal tangent makes possible homoclinic or heteroclinic bifurcations to take place.

At the saddle point $x = 0$, for an unperturbed system (Fig. 1), the system velocity reaches zero in velocity $y = 0$ (for infinite time $t = \pm\infty$) so the total energy has only its potential part. In this paper, the homoclinic case is be study.

Transforming Eqs. (3, 4), for a closed nodal energy ($H = 0$) and for $\gamma < 0, \lambda > 0$ we get the following expression for velocity:

$$y = \frac{dx}{dt} = \sqrt{2\left(-\frac{\gamma}{2}x^2 - \frac{\lambda}{4}x^4\right)}. \quad (7)$$

Now one can perform integration over x :

$$t - t_0 = \pm \int \frac{dx}{x\sqrt{-\gamma - \frac{\lambda}{2}x^2}}, \quad (8)$$

where t_0 represents an integration constant. Finally, we get so called homoclinic orbits (Fig. 2):

$$\begin{aligned} x_h &= \pm \sqrt{\frac{-2\gamma}{\lambda}} \operatorname{sech}(\sqrt{-\gamma}(t - t_0)) \\ y_h &= \pm \sqrt{\frac{2}{\lambda}} \gamma \operatorname{sech}(\sqrt{-\gamma}(t - t_0)) \tanh(\sqrt{-\gamma}(t - t_0)), \end{aligned} \quad (9)$$

where ‘+’ and ‘-’ signs are related to left – and right + sign orbits, respectively (Fig. 2). Note, the central saddle point $x_0 = 0$ is reached in time t corresponding to $+\infty$ and $-\infty$ respectively.

We apply the Melnikov method to our system in order to find the necessary criteria for the existence of homoclinic bifurcations and chaos. The Melnikov integral is defined as

$$M(t_0) = \int_{-\infty}^{+\infty} f(x_h, y_h) \wedge g(x_h, y_h) dt, \quad (10)$$

where the corresponding differential form f means the gradient of unperturbed hamiltonian while g is a perturbation from Eq. (6) after to put $\alpha = \epsilon\alpha$ and $F = \epsilon F$. Eq. (10) can be rewritten as follows:

$$\begin{aligned} M^\pm(t_0) &= -\mu \int y_h^2 dt + \mu \int y_h^4 dt - k_1 \int x_h y_h^2 dt - \beta \int y_h^3 dt - \\ &k_2 \int x_h y_h^3 dt - \alpha \int x_h y_h \cos \Omega(t + t_0) dt + \\ &F \int y_h \cos \Omega(t + t_0) dt, \end{aligned} \quad (11)$$

where t_0 is the cross-section time of the Poincare map and t_0 can be interpreted as the initial time of the forcing term. After substituting the equations of the homoclinic orbits x_h and y_h given in Eq. (9) into Eq. (11) and evaluating the corresponding integral, we obtain the Melnikov function given by

$$M^\pm(t_0) = -\mu I_0 + \mu I_1 - k_1 I_2 - \beta I_3 - k_2 I_4 - \alpha \sin \Omega t_0 I_5 + F \sin \Omega t_0 I_6, \quad (12)$$

where

$$\begin{aligned}
I_0 &= \frac{2\gamma^2}{\lambda} \int_{-\infty}^{+\infty} \operatorname{sech}^2(\sqrt{-\gamma}t) \tanh^2(\sqrt{-\gamma}t) dt, \\
I_1 &= \frac{4\gamma^4}{\lambda^2} \int_{-\infty}^{+\infty} \operatorname{sech}^4(\sqrt{-\gamma}t) \tanh^4(\sqrt{-\gamma}t) dt, \\
I_2 &= \pm \frac{2\gamma^2}{\lambda} \sqrt{\frac{-2\gamma}{\lambda}} \int_{-\infty}^{+\infty} \operatorname{sech}^3(\sqrt{-\gamma}t) \tanh^2(\sqrt{-\gamma}t) dt, \\
I_3 &= \pm \frac{2\gamma^3}{\lambda} \sqrt{\frac{2}{\lambda}} \int_{-\infty}^{+\infty} \operatorname{sech}^3(\sqrt{-\gamma}t) \tanh^3(\sqrt{-\gamma}t) dt, \\
I_4 &= \frac{4\gamma^3}{\lambda^2} \sqrt{-\gamma} \int_{-\infty}^{+\infty} \operatorname{sech}^4(\sqrt{-\gamma}t) \tanh^3(\sqrt{-\gamma}t) dt, \\
I_5 &= \frac{2\gamma}{\lambda} \sqrt{-\gamma} \int_{-\infty}^{+\infty} \operatorname{sech}^2(\sqrt{-\gamma}t) \tanh(\sqrt{-\gamma}t) \sin \Omega t_0 dt, \\
I_6 &= \pm \gamma \sqrt{\frac{2}{\lambda}} \int_{-\infty}^{+\infty} \operatorname{sech}(\sqrt{-\gamma}t) \tanh(\sqrt{-\gamma}t) \sin \Omega t_0 dt. \quad (13)
\end{aligned}$$

After evaluation of these elementary integrals (see Appendix), the Melnikov function is computed.

$$\begin{aligned}
M^\pm(t_0) &= \frac{4\mu\gamma\sqrt{-\gamma}}{3\lambda} - \frac{16\mu\gamma^3\sqrt{-\gamma}}{35\lambda^2} \mp \frac{\pi k_1\gamma^2}{8} \left(\frac{2}{\lambda}\right)^{\frac{3}{2}} \mp \\
&\frac{23}{70}\pi\Omega F \sqrt{\frac{2}{\lambda}} \operatorname{sech}\left(\frac{\pi\Omega}{2\sqrt{-\gamma}}\right) \sin \Omega t_0 - \frac{\pi\alpha\Omega^2}{2\lambda\sqrt{-\gamma}} \operatorname{cosech}\left(\frac{\pi\Omega}{2\sqrt{-\gamma}}\right) \sin \Omega t_0. \quad (14)
\end{aligned}$$

It is known, that the intersections of the homoclinic orbits are the necessary conditions for the existence of chaos. The Melnikov function theory measures the distance between the perturbed stable and unstable manifolds in the Poincaré section. If $M^\pm(t_0)$ has a simple zero, then a homoclinic bifurcation occurs, signifying the possibility of chaotic behavior. This means that only necessary conditions for the appearance of strange attractors are obtained from the Poincaré–Melnikov–Arnold analysis, and therefore one has always the chance of finding the sufficient conditions for the elimination of even transient chaos. Then the necessary condition for which the invariant manifolds intersect themselves is given by

$$\begin{aligned}
\mu_{cr} &= \frac{\lambda^2}{4\gamma\sqrt{-\gamma}\left(\frac{1}{3} - \frac{4\gamma^2}{35}\right)} \times \\
&\left[\frac{\pi\alpha\Omega^2}{2\lambda\sqrt{-\gamma}} \operatorname{cosech}\left(\frac{\pi\Omega}{2\sqrt{-\gamma}}\right) \pm \frac{23}{70}\pi\Omega F \sqrt{\frac{2}{\lambda}} \operatorname{sech}\left(\frac{\pi\Omega}{2\sqrt{-\gamma}}\right) \pm \frac{\pi k_1\gamma^2}{8} \left(\frac{2}{\lambda}\right)^{\frac{3}{2}} \right] \quad (15)
\end{aligned}$$

Above this value $\mu \geq \mu_{cr}$ the system transit through a global homoclinic bifurcation which is a necessary condition for appearance of chaotic vibrations.

This implies that if the perturbation is sufficiently small, the reduced Eq. (6) has transverse homoclinic orbits resulting in possible chaotic dynamics. We study the chaotic threshold as a function of only the frequency parameter Ω . A typical plot of μ against Ω is shown in Fig. 3, in which the critical homoclinic bifurcation curves are plotted versus the frequency parameter Ω . The threshold of chaotic motion increases

with the increasing of the external amplitude μ (Fig. 3). The region below the homoclinic bifurcation curve corresponding to $F = 0.3$ (region *I*) of Fig. 3) represents the periodic orbits. When μ crosses its first critical value, a homoclinic bifurcation takes place, so that a hyperbolic Cantor set appears in a neighborhood of the saddles (regions *II*) and *III*) of Fig. 3). The dynamics should therefore be chaotic only for large values of the damping. At the same time, when $F = 0.5$ (regions *I*) and *II*) of Fig. 3) it represents the periodic orbits, while the dynamics should therefore be chaotic in the region *III*). Fig. 4 represents the effect of different amplitude parameters values on critical amplitude μ versus frequency showing chaotic regions. When $\alpha = 0$ and $k_1 = 0$ the necessary condition for which the invariant manifolds intersect themselves corresponding exactly to the condition which is obtained by Siewe Siewe and al. for Rayleigh-Duffing oscillator [2] (see Fig. 4 (a)). Figs. 4 (b), (c) and (d) show respectively hybrid quadratic nonlinearity, amplitude of excitation parameter and these two parameters simultaneous effect on critical amplitude μ_{cr} for $F = 0.5$. In these case, we noticed that the parameters k_1, α and F are several effect on melnikov critical amplitude which show when chaotic behavior appear in the modified Rayleigh-Duffing. Critical amplitude increases with the increasing of the parameter k_1 (see Figs. 4 (b)) but with α the critical amplitude are two extrema which show the effect of parametric excitation.

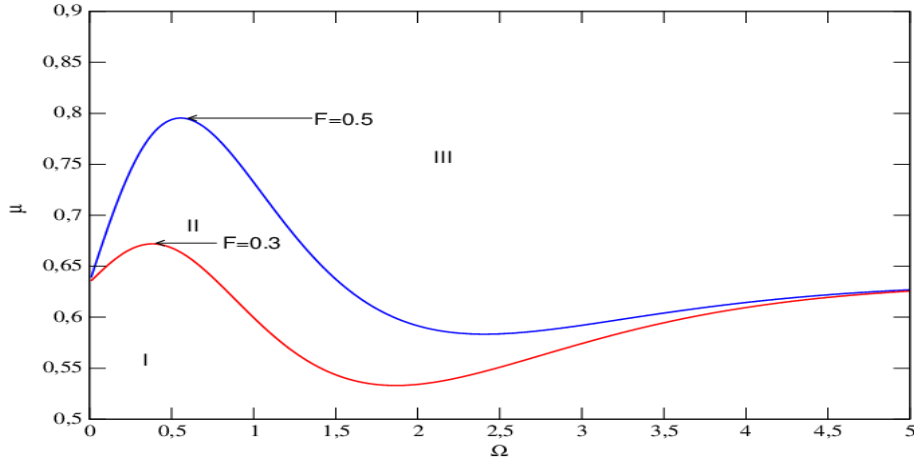


Figure 3: Critical amplitude μ versus frequency for two different external amplitude parameters values.

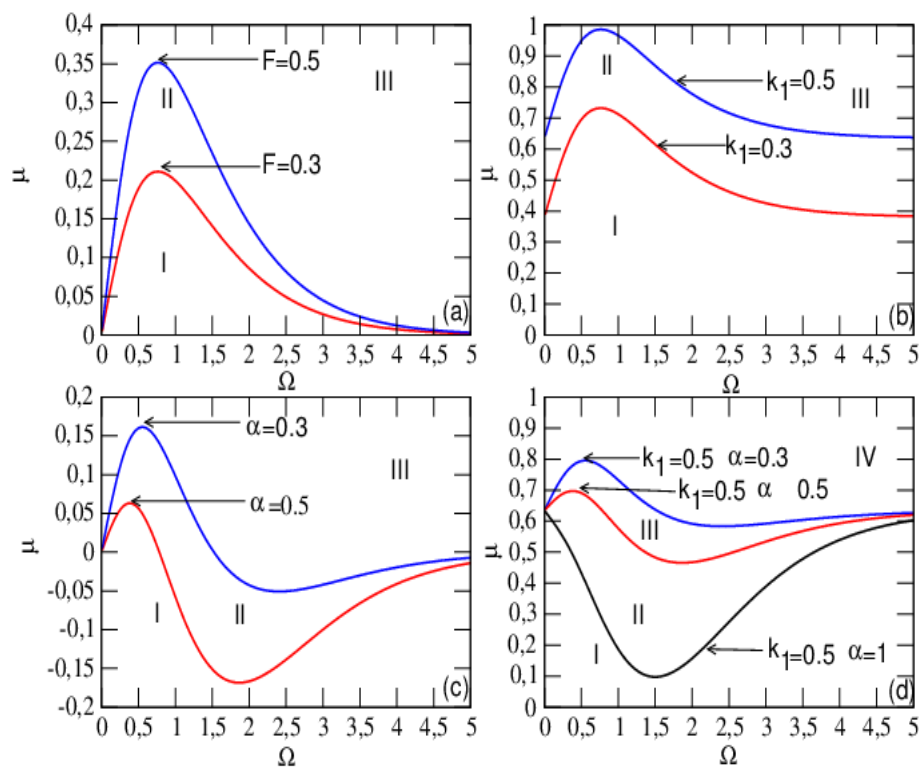


Figure 4: Effect of different amplitude parameters values on critical amplitude μ versus frequency showing chaotic regions.

4 Bifurcation analysis, phase portraits and fractal basins

In this part, we study the behavior of the system given by Eq.1 as a function of the damping parameter for different values of the external perturbation. The bifurcation diagram and the maximal Lyapunov exponents have been represented for the variable x , and they can be seen in Fig.5. A positive Lyapunov exponent for a bounded attractor is usually a sign of chaos. We want to check the threshold of the external amplitude for the onset of possible chaos obtained in Section 3. For $\Omega = 1$, the critical value of the external force has been obtained numerically for $F_{cr} = 0.5$. Above this value, numerical simulations have been carried out for the selected parameter values $F = 0.5$ (see Figs.5 (a) and (c)) and $F = 0.6$ (see Figs. 5(b) and (d)). From these figures, one can see that the thresholds of damping amplitude for the onset of chaos increase when the external amplitude increases above F_{cr} . After the chaotic motion in the small domain of μ ($[0, 0.085]$ for $F = 0.5$ and $[0, 0.13]$ for $F = 0.6$), the Lyapunov exponent changes from a negative value to a positive value when μ increases, signifying the appearance of homoclinic chaos motion. From Figs. 3 and 5, we can noticed that the Melnikov critical value μ_{cr} obtained in Section 3 is confirmed by numerical simulations. The phase portrait of chaotic and periodic orbits have been plotted in Fig. 7 with parameters of Fig.5. Clearly, we noticed that periodic appear when $\mu = 0.085$ and persist in means forms and is destroyed when this parameter is increasing which indicate the homoclinic chaos is appeared. Fig.6 illustrate the bifurcation diagram and the maximal Lyapunov exponents of our system when the modified parameters equals 0 ($\alpha = 0, \beta = 0, k_1 = 0, k_2 = 0$) and its corresponding phase portrait have been plotted in Fig.8. These figures show that our results coincide exactly with the results when the modified parameters equals 0 which are obtained for Rayleigh-Duffing by Siewe Siewe and al.(see [2]). The effect of nonlinear damping parameters, parametric excitation and external forced amplitude are also seeked through these figures.

A basin of attraction is defined as the set of points taken as initial conditions, that are attracted to a fixed point or an invariant set. The basin of attraction in this case signals the points in phase space that are attracted to a safe oscillation within the potential well, and the set of points that escape outside the potential well to the infinity. In order to verify the analytical results obtained in the previous sections, we have numerically integrated the system by using a fourth order Runge–Kutta in order to investigate the homoclinic chaos in our model. We want to study what is the effect of using the nonlinear damping terms on the equation of the oscillator and how the basins of attraction are affected as the coefficient parameter μ is varied. To show the fractal structure, we consider the case of the bifurcation close to the resonance since it may undergo the limit cycles in the system. We see through from Figs.9, 10, 11, 12, 13, 14, the basin boundaries become fractal, which means that the damping parameter value μ has contributed to the fractalization of the boundaries, with the corresponding uncertainty associated to this fact. For instance, as this control parameter increases above this critical value, the regular shape of basin of attraction is destroyed and the fractal behavior becomes more and more visible (see Fig.12 and 13). Such fractal boundaries indicate that whether the system is attracted to one or the other periodic attractor may be very sensitive to initial conditions. It is also found that even if μ is increased beyond the analytical critical value for the homoclinic bifurcation, it is still possible that the final steady motion could be periodic rather than chaotic. These results confirme our analytical result. Finally, we prove through from Figs. 13 and 14 the modified parameters of habitually Rayleigh-Duffing oscillator are very effect on chaotic motions of this system.

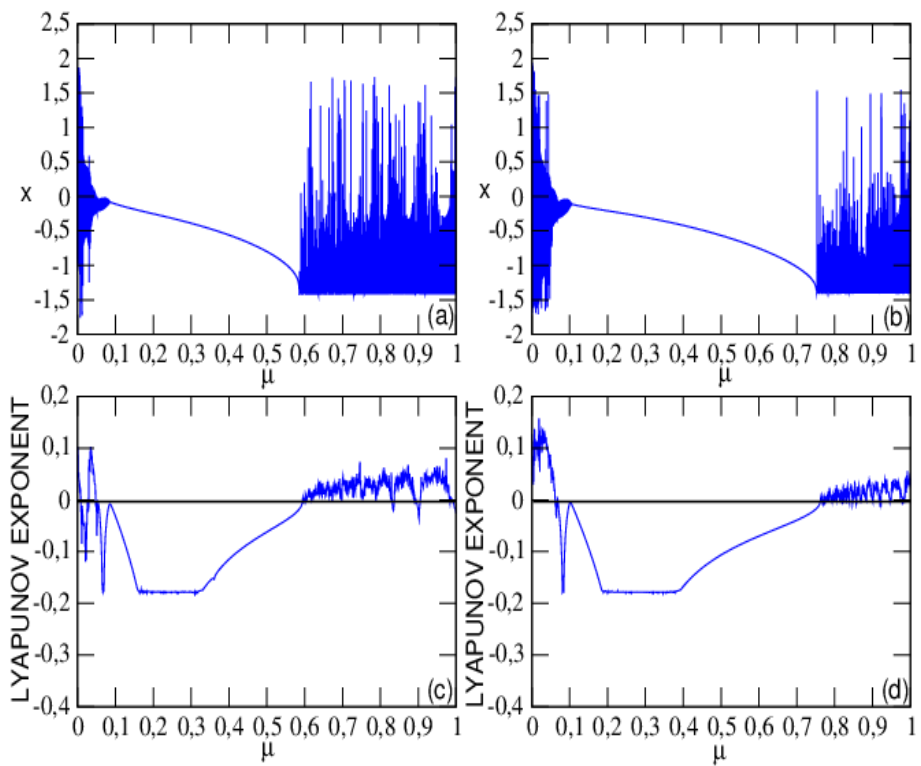


Figure 5: Bifurcation diagram and corresponding Maximal Lyapunov exponent of Modified Rayleigh-Duffing oscillator equation versus μ with parameters of Fig. 3; $(a, c) F = 0.5$, $(b, d) F = 0.6$.

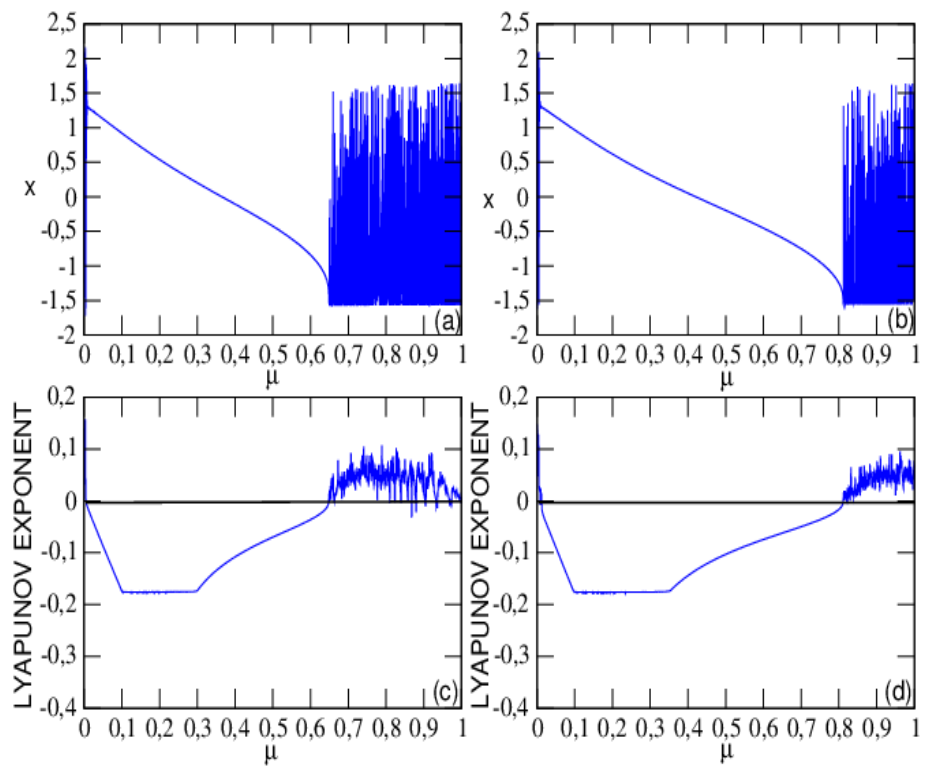


Figure 6: Bifurcation diagram and corresponding Maximal Lyapunov exponent of Modified Rayleigh-Duffing oscillator equation versus μ when the modified parameters equals to 0 with parameters of Fig. 4(a); (a, c) $F = 0.5$, (b, d) $F = 0.6$.

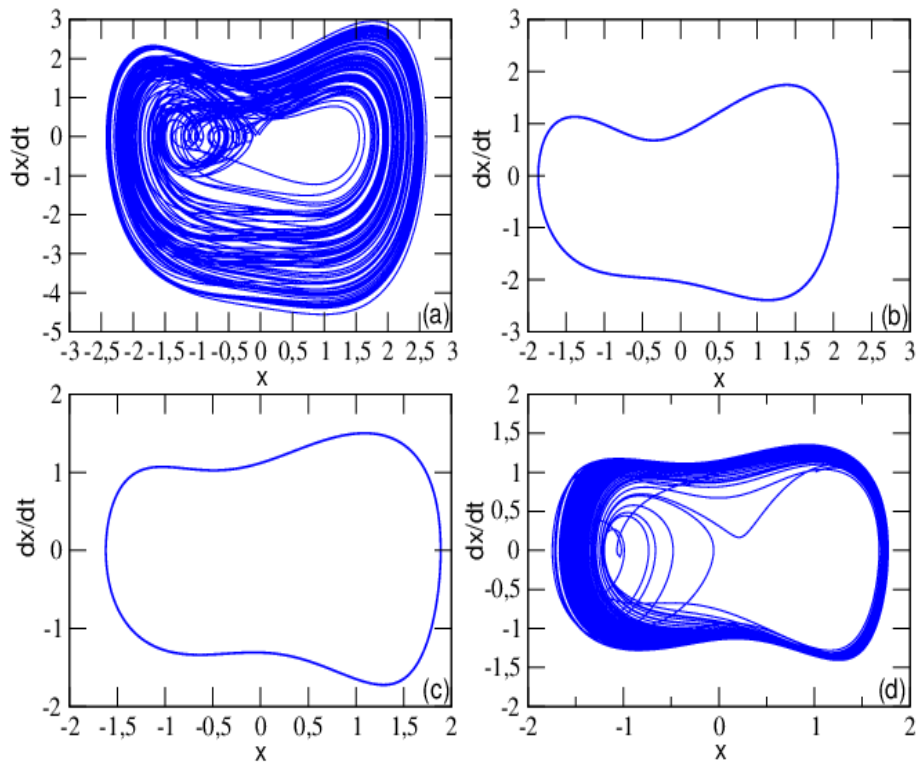


Figure 7: Phase portraits corresponding to Modified Rayleigh-Duffing oscillator with parameters of Fig.5; (a) chaotic orbit $\mu = 0.0001$, (b) period-1 orbit $\mu = 0.1$, (c) period-1 orbit $\mu = 0.5$, (d) chaotic orbit $\mu = 0.8$.

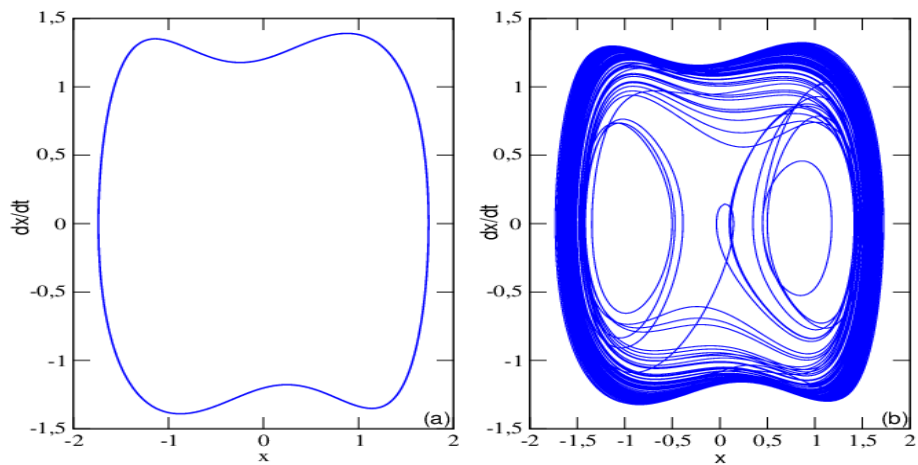


Figure 8: Phase portraits corresponding to Modified Rayleigh-Duffing oscillator when the modified damping parameters equals to 0 with parameters of Fig.6; (a) period-1 orbit $\mu = 0.5$, (b) chaotic orbit $\mu = 0.695$.

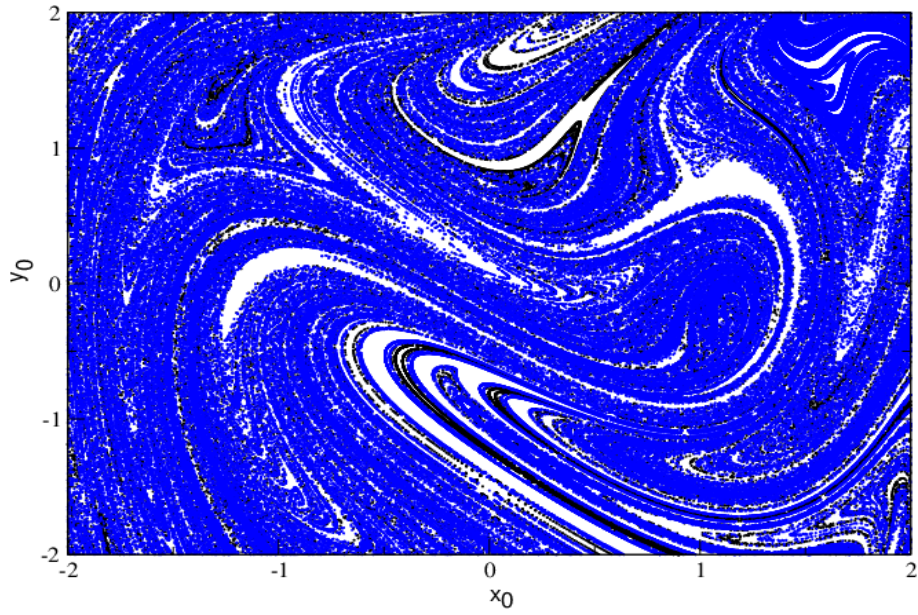


Figure 9: Basin of attraction corresponding to the system with $\mu = 0.0001$, the others parameters are: $\gamma = -1, \lambda = 1, \alpha = 0.3, \beta = 0.05, \Omega = 1, \epsilon = -1, k_1 = 0.5, k_2 = 0.05$ and $F = 0.5$.

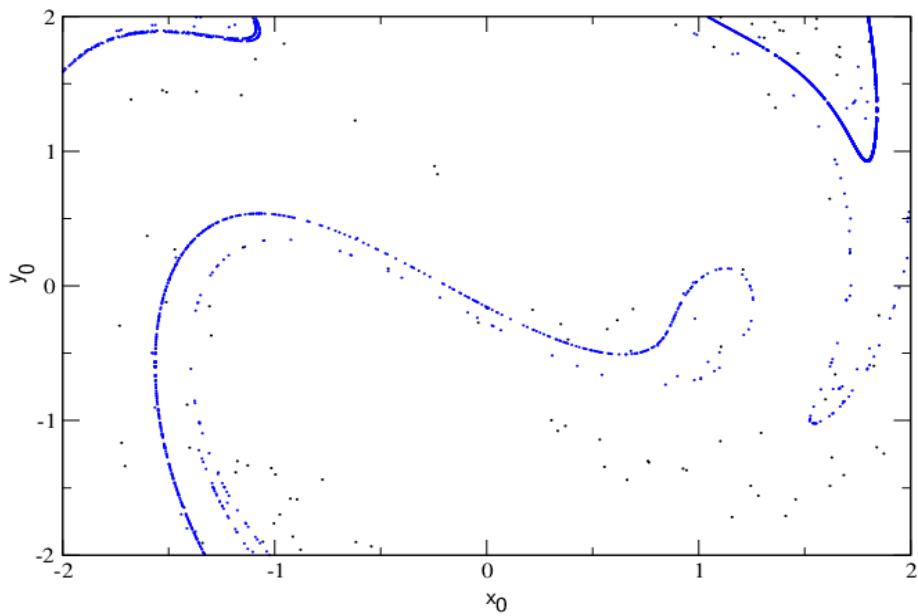


Figure 10: Basin of attraction corresponding to the system with $\mu = 0.045$, and the parameters of 9.

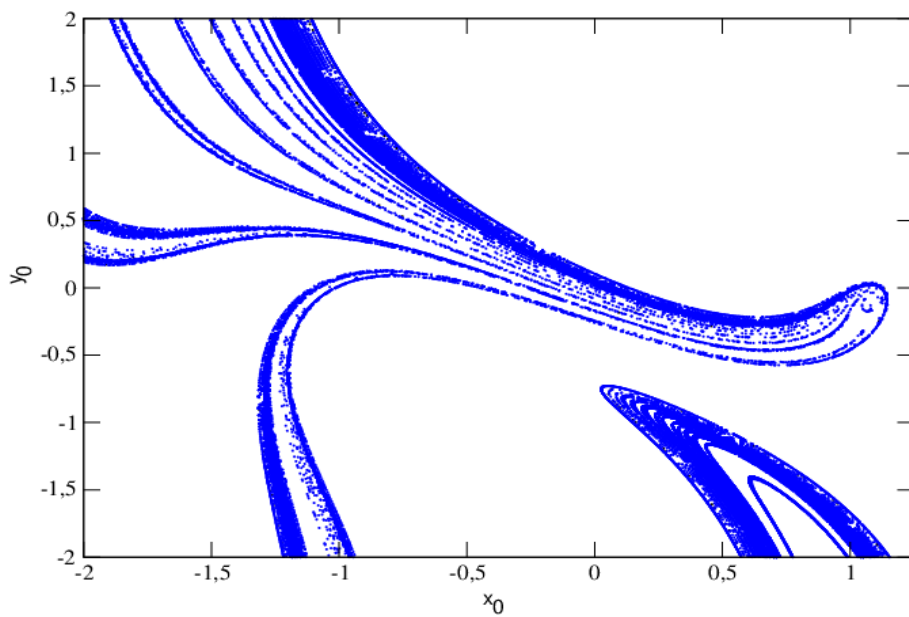


Figure 11: Basin of attraction corresponding to the system with $\mu = 0.6$, and the parameters of 9.

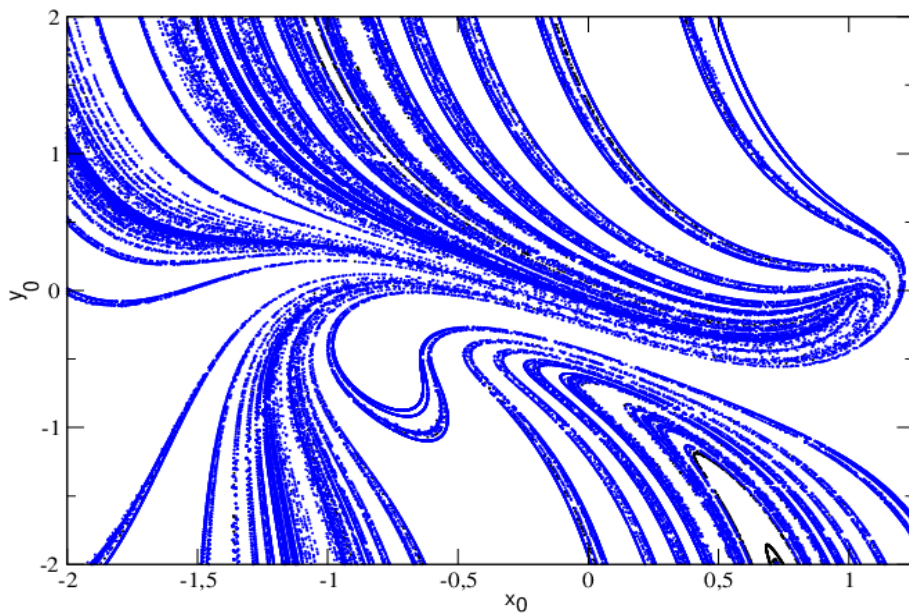


Figure 12: Basin of attraction corresponding to the system with $\mu = 0.8$, and the parameters of 9.

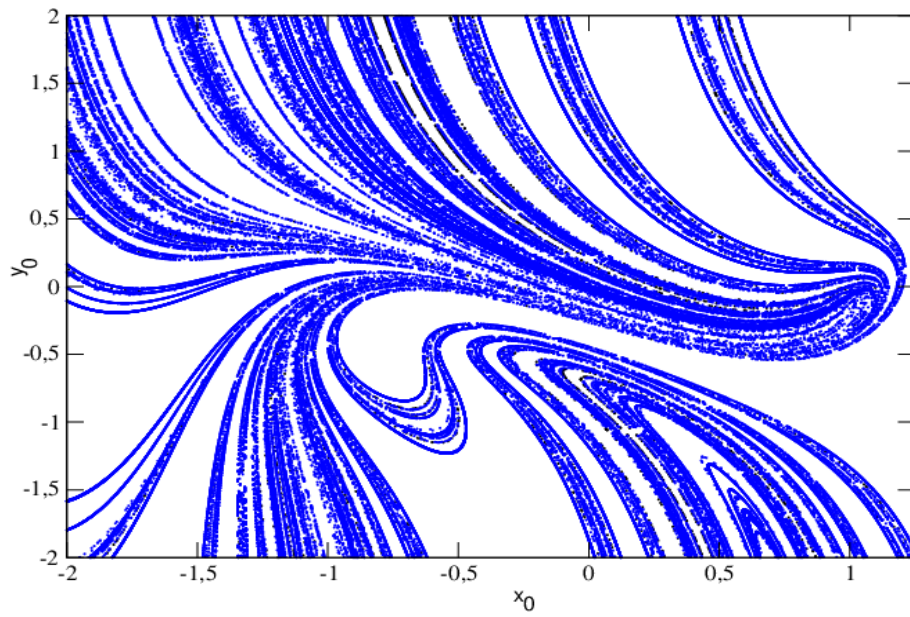


Figure 13: Basin of attraction corresponding to the system with $\mu = 0.85$, and the parameters of 9.

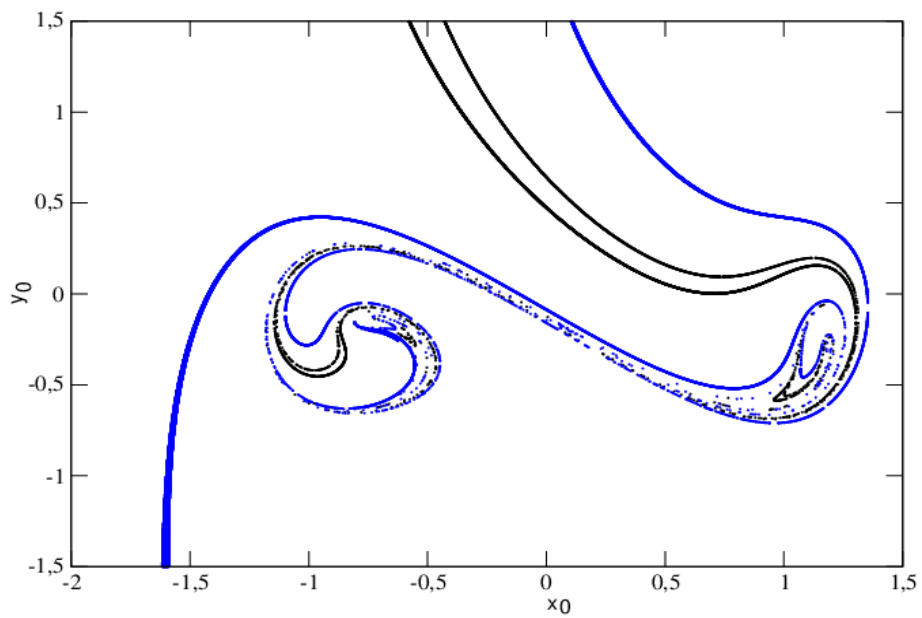


Figure 14: Basin of attraction corresponding to the system with $\mu = 0.6$, and the parameters of 8.

5 Conclusion

In this paper, we have studied conditions of a global homoclinic bifurcation in a double well potential modified Rayleigh-Duffing system with pure cubic nonlinear damping coefficient term. Using the Melnikov method we have got the analytical formula for transition to chaos in a one degree of freedom, system subjected to self-excitation term with a non-symmetric stiffness with parametric excitation. In our case this effect is mutually introduced through the modified Rayleigh-Duffing damping and parametric excitation terms. The transition boundaries in the parameter space are obtained, which divide the space into different regions. In each region, the solutions are explored theoretically and numerically. The critical value of damping coefficient μ under which the system oscillates chaotically has been estimated, in the first step by means of the Melnikov method and later confirmed by calculating the corresponding Lyapunov exponent, bifurcation diagrams, and basin of attractions. Results were given for external periodic perturbation. By means of the basin of attraction, we have shown that for certain regions of parameter space, the deterministic system driven harmonically experiences behaviors that may be chaotic or non-chaotic. The Melnikov method, is sensitive to a global homoclinic bifurcation and gives a necessary condition when the damping coefficient $\mu = \mu_{cr1}$ is larger than the critical homoclinic bifurcation values. Our analytical results are consistent with direct computations on homoclinic orbits. It is also investigated the effect of unpure quadratic nonlinear damping and parametric excitation amplitude on chaotic behavior through the melnikov criteria and attraction basin.

Acknowledgments

The authors thank IMSP-UAC and Benin government for financial support.

Appendix A

Evaluation of the integrals from I_0 , to I_6 is straightforward. After substitution $x_h(t)$, and $y_h(t)$ (Eq. (9)) we have:

$$\begin{aligned} I_0 &= \frac{2\gamma^2}{\lambda} \int_{-\infty}^{+\infty} \operatorname{sech}^2(\sqrt{-\gamma}t) \tanh^2(\sqrt{-\gamma}t) dt \\ &= \frac{2\gamma^2}{\lambda} \int_{-\infty}^{+\infty} \frac{\tanh^2(\sqrt{-\gamma}t)}{\cosh^2(\sqrt{-\gamma}t)} dt. \end{aligned} \quad (16)$$

and simple algebraic manipulations:

$$\tau = t\sqrt{-\gamma}, \quad \tanh \tau = \xi, \quad (17)$$

we obtain

$$I_0 = \frac{2\gamma^2}{\lambda\sqrt{-\gamma}} \int_{-1}^1 \xi^2 d\xi. \quad (18)$$

Finally the result of one has a following expression:

$$I_0 = \frac{-4\gamma\sqrt{-\gamma}}{3\lambda}. \quad (19)$$

After same algebraic manipulations, I_1 , and I_4 become finally

$$I_1 = -\frac{16\gamma^3\sqrt{-\gamma}}{35\lambda^2} \quad (20)$$

and

$$I_4 = 0. \quad (21)$$

On the the hand the integrals I_2 and I_3 can be evaluated by using following expressions:

$$\begin{aligned} \int \frac{\sinh^p \tau}{\cosh^{2n+1} \tau} d\tau &= \frac{\sinh^{p+1} \tau}{2n} \times \\ &[sech^{2n} \tau + \sum_{k=1}^{n-1} \frac{(2n-p-1)(2n-p-3)\dots(2n-p-2k+1)}{2^k(n-1)(n-2)\dots(n-k)} sech^{2n-2k}] + \\ &\frac{(2n-p-1)(2n-p-3)\dots(3-p)(1-p)}{2^n n!} \int \frac{\sinh^p \tau}{\cosh \tau} d\tau \end{aligned} \quad (22)$$

$$\begin{aligned} \int \frac{\sinh^p \tau}{\cosh^{2n} \tau} d\tau &= \frac{\sinh^{p+1} \tau}{2n} \times \\ &[sech^{2n-1} \tau + \sum_{k=1}^{n-1} \frac{(2n-p-2)(2n-p-4)\dots(2n-p-2k)}{(2n-3)(2n-5)\dots(2n-2k-1)} sech^{2n-2k-1}] + \\ &\frac{(2n-p-2)(2n-p-4)\dots(-p+2)(-p)}{(2n-1)!!} \int \sinh^p \tau d\tau \end{aligned} \quad (23)$$

$$\int \frac{\sinh^2 \tau}{\cosh \tau} d\tau = \sinh \tau - \arctan(\sinh \tau), \quad (24)$$

and

$$\int \sinh^3 \tau d\tau = \frac{1}{3} \cosh^3 \tau - \cosh \tau \quad (25)$$

With these expressions, the finite values of I_2 and I_3 are:

$$I_3 = \pm \frac{\pi\gamma^2}{4\lambda} \sqrt{\frac{2}{\lambda}} \quad (26)$$

and

$$I_4 = 0. \quad (27)$$

Now, we evaluate I_5 and I_6 .

$$I_5 = \frac{2\gamma}{\lambda} \sqrt{-\gamma} \int_{-\infty}^{+\infty} sech^2(\sqrt{-\gamma}t) \tanh(\sqrt{-\gamma}t) \cos \Omega(t+t_0) dt, \quad (28)$$

$$I_5 = \frac{2\gamma\sqrt{-\gamma}}{\lambda} \sin \Omega t_0 \int_{-\infty}^{+\infty} \frac{\tanh \tau}{\cosh^2 \tau} \sin \frac{\Omega\tau}{\sqrt{-\gamma}} dt \quad (29)$$

We put

$$I_5^A = \int_{-\infty}^{+\infty} \frac{\tanh \tau}{\cosh^2 \tau} \sin \frac{\Omega \tau}{\sqrt{-\gamma}} dt \quad (30)$$

This integrale can be calculated by using the residue theorem

$$\oint f(z) dz = 2\pi i \sum_{k=1}^N \text{Res}[f(z), z_k], \quad (31)$$

where

$$\text{Res}[f(z), z_k] = \frac{1}{(m-1)!} \lim_{z \rightarrow z_k} \frac{d^{m-1}}{dz^{m-1}} [(z - z_k)^m f(z)]. \quad (32)$$

In our case,

$$f(z) = 4 \frac{\exp(z) - \exp(-z)}{(\exp(z) + \exp(-z))^3} \exp \frac{i\Omega z}{\sqrt{-\gamma}}, \quad (33)$$

where on the real axis (Fig. 15) $\text{Re} z = \tau$:

$$\text{Im} f(z) = \frac{\tanh \tau}{\cosh^2 \tau} \sin \left(\frac{\Omega \tau}{\sqrt{-\gamma}} \right). \quad (34)$$

The multiplicity of each pole of the complex function $f(z)$ (Eq. (33):

$$z_k = \left(\frac{\pi}{2} + \pi k \right) i \quad \text{for } k = 1, 2, \dots \quad (35)$$

can be easily determined as $m = 3$. After summation of all poles (Fig. 15) we get:

$$I_5^A = \frac{2\pi\Omega^2}{\gamma} \frac{\sin\left(\frac{\Omega z_0}{\sqrt{-\gamma}}\right)}{\sinh\left(\frac{\Omega\pi}{2\sqrt{-\gamma}}\right)} \quad (36)$$

Finally, the result of the above analysis can be written:

$$I_5 = \frac{4\pi\Omega^2}{\lambda} \frac{\sin(\Omega t_0)}{\sinh\left(\frac{\Omega\pi}{2\sqrt{-\gamma}}\right)} \quad (37)$$

Integral I_6 is calculated with the same algebraic manipulations and the can be written as follows:

$$I_6 = \mp \frac{23}{70} \pi \Omega \sqrt{\frac{2}{\lambda}} \text{sech}\left(\frac{\pi\Omega}{2\sqrt{-\gamma}}\right) \sin \Omega t_0. \quad (38)$$

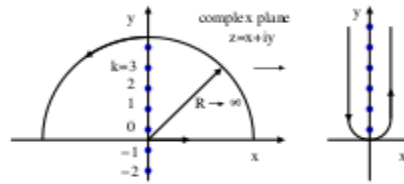


Figure 15: Deformed contour integration schema and imaginary poles.

References

- [1] Valery Tereshko, *Control and Identification of Chaotic Systems by Altering the Oscillation Energy*, Chaotic Systems, 2011 University of the West of Scotland United Kingdom.
- [2] M. Siewe Siewe, Hongjun Cao, Miguel A.F. Sanjuán, *Effect of nonlinear dissipation on the basin boundaries of a driven two-well Rayleigh–Duffing oscillator*, Chaos, Solitons and fractals 39 (2009) 1092–1099.
- [3] M. Siewe Siewe, Hongjun Cao, Miguel A.F. Sanjuán, *On the occurrence of chaos in a parametrically driven extended Rayleigh oscillator with three-well potential*, Chaos, Solitons and fractals 41 (2009) 772–782.
- [4] B.R. Nana Nbandjo, R. Tchoukuegno, P. Wofo, *Active control with delay of vibration and chaos in a double-well Duffing oscillator*, Chaos, Solitons and Fractals 18 (2003) 345–353.
- [5] B.R. Nana Nbandjo, Y. Salissou, P. Wofo, *Active control with delay of vibration and chaos in a double-well Duffing oscillator*, Chaos, Solitons and Fractals 23 (2005) 809–816.
- [6] Wajdi M. Ahmad, J.C. Sprott, *Chaos in fractional-order autonomous nonlinear systems*, Chaos, Solitons and Fractals 16 (2003) 339–351
- [7] Amir H. Davaie-Markazi and H. Sohanian–Haghighi, *Chaos Analysis and Control in AFM and MEMS Resonators*, Chaotic Systems www.intechopen.com
- [8] Valery Tereshko, *Control and Identification of Chaotic Systems by Altering the Oscillation Energy*, chaotic systems www.intechopen.com
- [9] A. Venkatesan and M. Lakshmanan, *Bifurcation and chaos in the double well Duffing- van der Pol oscillator: Numerical and analytical studies*, arXiv:chaodyn/9709013v1 11 sep 1997, Typeset using REVTEX.
- [10] Grzegorz Litak, Marek Borowiec, Arkadiusz Syta, Kazimierz Szabelski, *Transition to Chaos in the Self-Excited System with a Cubic Double Well Potential and Parametric Forcing*, Chaos, Solitons and Fractals 40 (2009) 2414–2429.
- [11] C. A. Kitio Kwuimy and M. Belhaq *Effect of A Fast Harmonic Excitation on Chaotic Dynamic in a Van der Pol-Mathieu-Duffing Oscillator*, Int. J. of Appl. Math. and Mech. 8(10): 59-70.

- [12] V. Ravichandran, V. Chinnathambi, S. Rajasekar , Choy Heng Lai, *Effect of the shape of periodic forces and second periodic forces on horseshoe chaos in Duffing oscillator*, arXiv:0808.0406v1 [nlin.CD] 4 Aug 2008.
- [13] Wiggins S., *Introduction to applied nonlinear dynamical systems and chaos*, New York, Heidelberg, Berlin: Springer-Verlag; 1990.
- [14] Moon FC, Li GX, *Fractal basin boundaries and homoclinic orbits for periodic motion in a two-well potential*, Phys Rev Lett 1985;55:1439.
- [15] C. H. Miwadinou, L. A. Hinvi, A. V. Monwanou and J. B. Chabi Orou, *Non-linear dynamics of plasma oscillations modeled by a forced modified Van der Pol-Duffing oscillator*, arXiv:1308.6132v1 [physics.flu-dyn] 28 Aug 2013.
- [16] C. H. Miwadinou, A. V. Monwanou and J. B. Chabi Orou, *Parametrics resonances of a Forced Modified Rayleigh-Duffing Oscillator*, arXiv:1304.7176v1 [physics.flu-dyn] 26 Apr 2013.
- [17] Grzegorz Litak, Marek Borowiec, Michael I. Friswell, Kazimierz Szabelski, *Chaotic vibration of a quarter-car model excited by the road surface profile*, Communications in Nonlinear Science and Numerical Simulation 13 (2008) 1373–1383.
- [18] C. H. Miwadinou, A. V. Monwanou and J. B. Chabi Orou, *Active Control of the Parametric Resonance in the Modified Rayleigh-Duffing oscillator*, arXiv:1304.7176v1 [physics.flu-dyn] 26 Mar 2013.
- [19] Marek Borowiec and Grzegorz Litak, *Vibration of the Duffing Oscillator: Effect of Fractional Damping*, Shock and Vibration 14 (2007) 29–36 IOS Press
- [20] M. Siewe Siewe, F. M. Moukam Kakmeni, C. Tchawoua, and P. Wofo, *Nonlinear Response and Suppression of Chaos by Weak Harmonic Perturbation inside a Triple Well 6-Rayleigh Oscillator Combined to Parametric Excitations*, Journal of Computational and Nonlinear Dynamics, vol. 1 pp. 196-204, 2006.
- [21] Cao H, Seoane JM, Sanjuán MAF, *Symmetry-breaking analysis for the general Helmholtz–Duffing oscillator*, Chaos, Solitons and Fractals 2007;34:197–212.
- [22] Trueba JL, Baltanas JP, Sanjuán MAF, *A generalized perturbed pendulum*, Chaos, Solitons and Fractals 2003;15:911.
- [23] Sanjuán MAF, *The effect of nonlinear damping on the universal escape oscillator*, Int J Bifurcat Chaos 1999;9:735.
- [24] Munehisa S, Inaba N, Yoshinaga T, Kawakami H, *Bifurcation structure of fractional harmonic entrainments in the forced Rayleigh oscillator*, Electron Commun Jpn Part 3: Fundam Electron Sci 2004;87:30–40.
- [25] Marek Borowiec and Grzegorz Litak, *Transition to chaos and escape phenomenon in two-degrees-of-freedom oscillator with a kinematic excitation*, Nonlinear Dyn DOI 10.1007/s11071-012-0518-8